LBL-9125

FERMILAB-Pub-79/33-exp

C00-3072-95

Observation of J/ψ(3100) Production by 209-GeV Muons

A.R. Clark, K.J. Johnson, L.T. Kerth, S.C. Loken, T.W. Markiewicz,

P.D. Meyers, W.H. Smith, M. Strovink, and W.A. Wenzel

Physics Department and Lawrence Berkeley Laboratory,
University of California, Berkeley, California 94720

and

R.P. Johnson, C. Moore, M. Mugge, and R.E. Shafer

Fermi National Accelerator Laboratory,
Batavia, Illinois 60510

and

G.D. Gollin, F.C. Shoemaker, and P. Surko

Joseph Henry Laboratories, Princeton University,
Princeton, New Jersey 08544

Interactions of 209-GeV muons within a magnetized-steel calorimeter have produced 1000 ± 80 $\mu^+\mu^-$ pairs from J/ψ(3100) decay. Redundant systems of proportional and drift chambers maintained uniform acceptance and 9% mass resolution. Above 30 GeV, the cross section for ψ production by virtual photons is found to rise less steeply with energy than predicted by a QCD calculation. Its dependence on Q^2 fits the vector dominance form $(1+Q^2/M^2)^{-2}$ with M = 2.7 ± 0.5 GeV.

Traditionally, photon-hadron interactions have been discussed[1] within the framework of vector-meson dominance (VMD) at low Q^2, and in terms of the constituent structure of hadrons at higher Q^2. The production of $J/\psi(3100)$[2] by photons, if damped by a VMD propagator $(1+Q^2/m_\psi^2)^{-2}$, requires description over a range in Q^2 spanning both domains. Elements of quantum chromodynamics (QCD) have been used in calculations attempting to provide this description[3,4,5].

This Letter is based on 1000 ± 80 examples of μ Fe $\rightarrow \mu\psi X$, $\psi \rightarrow \mu^+\mu^-$, the first reported observation of ψ production by spacelike photons. The events are drawn from a sample of 16834 fully-reconstructed 3μ final states produced by 209-GeV muons at Fermilab. ψ production by real photons has been observed at Fermilab[6,7], SLAC[8], and Cornell[9].

The spectrometer in Fig. 1, in part described elsewhere[10], was illuminated by 4×10^{11} beam muons. Twelve percent of the data are reported here. The beam intensity ranged from 0.03 to 0.11 per 19-nsec RF period. For 3μ final states, the trigger demanded $\geq$ 3 hits in each of 3 consecutive trigger scintillator banks (Fig. 1). Events were vetoed by additional beam (halo) muons within 28(10) nsec. The trigger efficiency was uniform near the ψ mass, with a threshold below $\sim$1 GeV.

Beam tracks were momentum-analyzed by 2 separate upstream bends. Accepted outgoing tracks, registering $\geq$ 4 proportional chamber hits in 2 views and $\geq$ 3 hits in the third, were required to intersect at a common vertex optimized by iteration. The result of a combined fit to the track momentum and Coulomb scattering angle in each module was used to reject background hits. The 3μ events were subjected to a 1-constraint fit which conserved energy, including hadron shower energy. A Monte Carlo

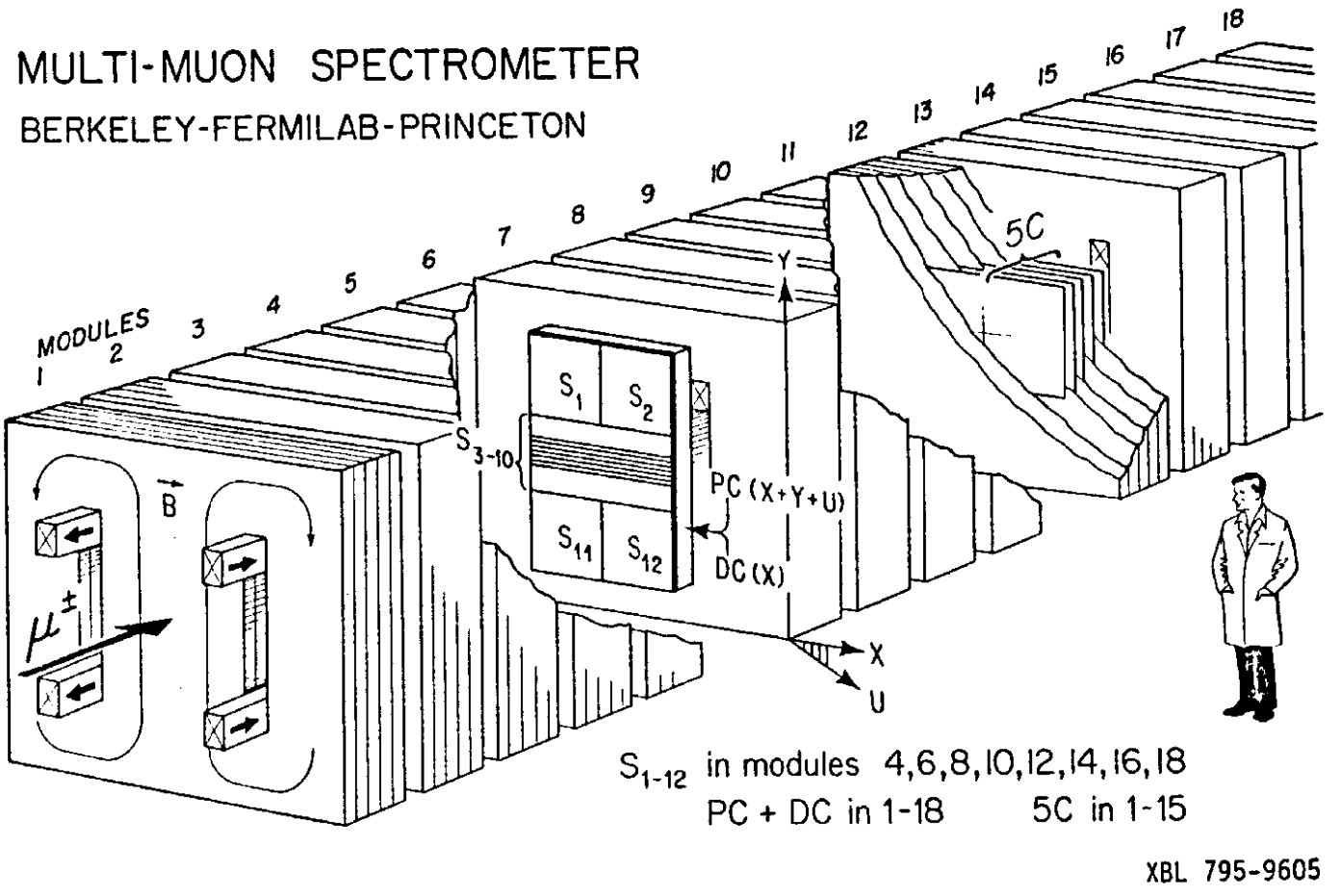

FIG.1. The spectrometer magnet, serving also as a target and hadron absorber, reaches 19.7 kgauss within a 1.8x1x16 m^3 fiducial volume. Over the central 1.4x1x16 m^3, the magnetic field is uniform to 3% and mapped to 0.2%. Eighteen pairs of proportional (PC) and drift chambers (DC), fully sensitive over 1.8x1 m^2, determine muon momenta typically to 8%. The PC's register coordinates at 30^o (u) and 90^o (y) to the bend direction (x) by means of 0.5-cm-wide cathode strips. Banks of trigger scintillators (S_1-S_{12}) occupy 8 of the 18 magnet modules. Interleaved with the 10-cm thick magnet plates in modules 1-15 are 75 calorimeter scintillators resolving hadron energy E_{had} with rms uncertainty $1.5E_{had}^{\frac{1}{2}}$ (GeV). Not shown upstream of module 1 are one PC and DC, 63 beam scintillators, 8 beam PC's,and 94 scintillators sensitive to accidental beam and halo muons.

program modeled the spectrometer, including detector resolutions and efficiencies, and scattering and energy-loss straggling in the steel plates. Using randomly sampled beam muons, it simulated interactions with nucleons in Fermi motion, or coherently with Fe nuclei. Shadowing and minimum-momentum transfer-squared ($|t|_{min}$) effects were included.

The mass spectrum of $\mu^+\mu^-$ pairs is exhibited in Fig. 2(a). If the two like-sign muons differed by more than a factor of 2 in energy, the unpaired muon was chosen to be the more energetic; otherwise, it was chosen to make the smaller laboratory angle with the beam track. This pairing algorithm retained 92% of the Monte Carlo ψ's in the mass peak, dispersing the remainder in a broad spectrum between 0.7 and 6 GeV, without producing important distortions in distributions of other variables.

The mass continuum, containing QED tridents, mispaired ψ's, and muonic decays of other particles, is subtracted to produce the peak in Fig. 2(b). The peak centroid is consistent with 3.1 GeV, and the width is consistent with the mean 9%-rms resolution predicted by Monte Carlo and by direct calculation for each event. The $\psi'(3685)$ is unresolved.

Data taken at low beam intensity, with interactions restricted to the upstream 8 spectrometer modules, were used for absolute normalization[11]. The total cross section is

$$\sigma/\text{nucleon}\ (\mu\ \text{Fe} \rightarrow \mu\psi X) = 0.76 \pm 0.22\ \text{nb},$$

allowing for the 7% $\psi \rightarrow \mu^+\mu^-$ branching fraction. Corrections (discussed below) for nuclear effects yield

$$\sigma(\mu N \rightarrow \mu\psi X) = 0.67 \pm 0.20\ \text{nb},$$

where the error is normalization uncertainty. A calculation[5] using the

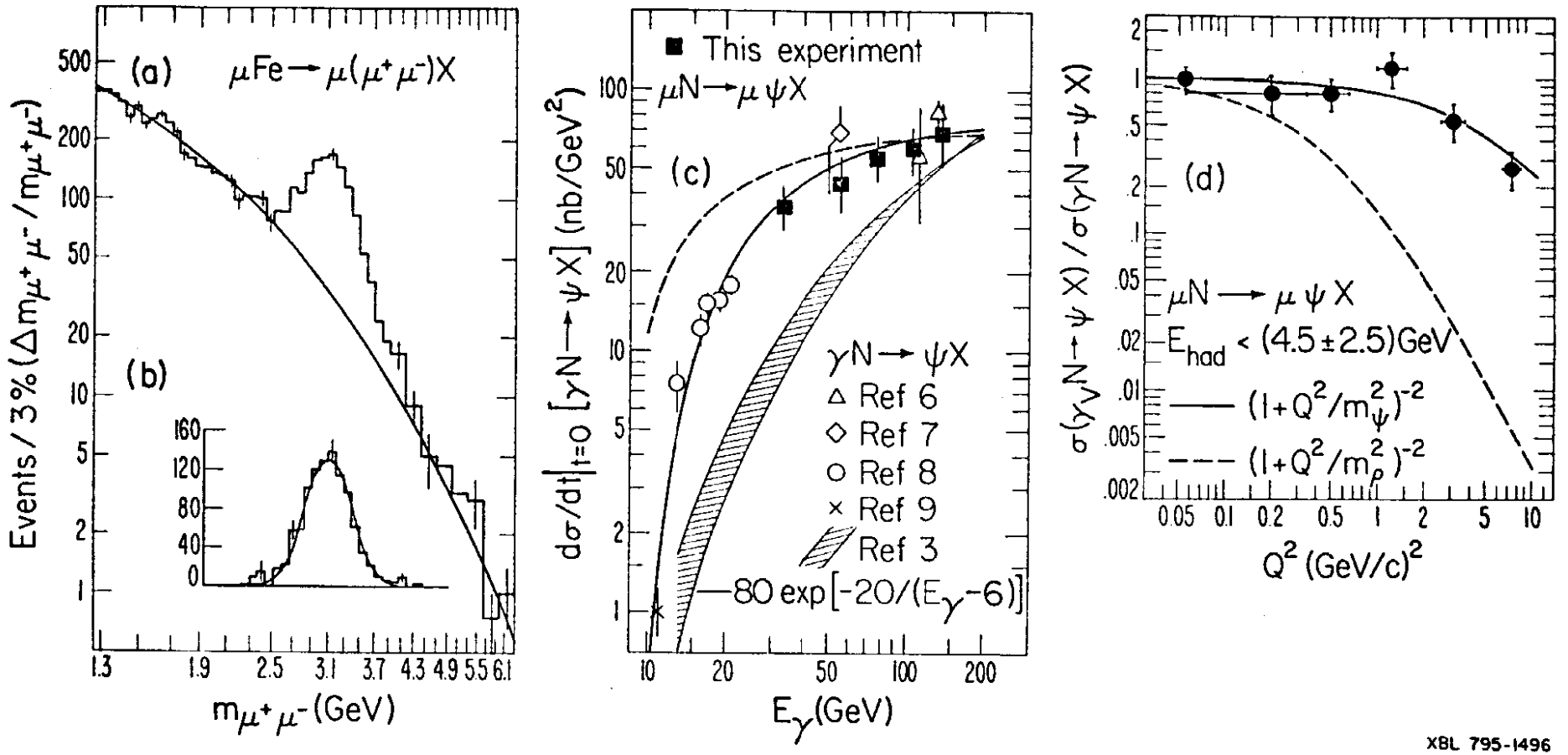

FIG.2. (a) Invariant mass spectrum of muoproduced $\mu^+\mu^-$. The curve is a representative fit to the continuum. Variations in the continuum parameterization contribute to the quoted errors on ψ yields. (b) ψ mass peak after continuum subtraction. The curve is a Gaussian centered at 3.1 GeV with rms width of 9%. (c) Energy-dependence of ψ photoproduction at t=0. The muoproduction points (squares) use an equivalent-photon approximation. Not indicated is their ±30% normalization error. (d) Q^2-dependence of ψ production by the equivalent-photon flux (Ref. 12). The data are normalized to 1 at the lowest Q^2 point. Horizontal error flags show typical Q^2 resolution.

photon-gluon-fusion diagram is consistent with this result.

Figures 2(c) and 2(d) exhibit the dependence of ψ production on photon energy (E_γ) and Q^2. Each of the muon data points is the result of a mass-continuum subtraction like that in Fig. 2(a-b). To suppress contamination from inelastic processes such as $\psi' \to \psi$ + hadrons, the calorimeter energy is required to be consistent with elastic ψ-production. Muon cross sections are converted to photon cross sections by extracting the equivalent flux[12] of transversely polarized photons. Neglect of any longitudinally-polarized photon cross section is consistent with the observed $\mu^+\mu^-$ angular distribution in the ψ c.m.

To make contact with other data[8] at small t, the t-dependence of the cross section is assumed to be

$$d\sigma/dt(\gamma\ Fe \to \psi X) = G(t)d\sigma/dt(\gamma N \to \psi N)(t=0)$$

$$G(t) = A_e^2 \exp(\alpha t) + A_e[(1-\varepsilon\delta)\exp(\beta t)+\varepsilon\delta\exp(\delta t)].$$

The coherent slope α, unresolved in the data, is set to 150 $(GeV/c)^{-2}$ based on lower-energy photon-nucleus measurements[13]. We take A_e=55.85x0.9 from electron-nucleus scattering[14] at $Q^2 \sim 0.5$. The choices β=3, δ=1, ε=1/8, in agreement with photoproduced ψ data[6], have been used in the Monte Carlo simulation to reproduce the experimental t distribution with a χ^2 of 5.9 for 6 degrees of freedom. With this t-dependence, the Monte Carlo is used to unfold acceptance, nuclear coherence, shadowing, and $|t|_{min}$ effects. The resulting γ-N cross section is divided by the integral $[(1-\varepsilon\delta)/\beta+\varepsilon)]$ = 5/12 of the incoherent term in G(t), and interpreted as $d\sigma(\gamma N)/dt(t=0)$. The parameters α, A_e, ε, β, and δ were varied over the range allowed by these and other data. The

TABLE I. Percent reduction in $d\sigma/dt(t=0)$ for ψ production by virtual photons, induced by variations in nuclear and nucleon parameters α $(GeV/c)^{-2}$, A_e, ε, β $(GeV/c)^{-2}$, and δ $(GeV/c)^{-2}$.

Parameter	α	A_e	ε	β	δ
Best value	150	50.27	1/8	3	1
Varied value	135	55.85	1/5	2.5	0.5
$\langle E_\gamma \rangle$ (GeV)					
34	3	11	10	12	5
56	5	12	9	10	4
77	5	13	8	9	3
106	5	13	7	8	3
140	5	14	7	8	3

E_γ-dependence of the result is shown in Table I to be insensitive to these variations.

Above 30 GeV, the cross section in Fig. 2(c) varies less steeply with E_γ than is predicted by a photon-gluon-fusion calculation[3] (shaded band). The broken line is the shape of the kinematic factor $(p^{\psi}_{c.m.}/p^{\gamma}_{c.m.})^2$. In the simplest VMD interpretation, the ratio of solid to broken lines in Fig. 2(c) gives the energy-dependence of the square of the ψ-nucleon total cross section.

The shallow Q^2-dependence in Fig. 2(d) is fit by $(1+Q^2/M^2)^{-2}$ with $M = 2.7 \pm 0.5$ GeV. This is interpreted within VMD as the mass of the ψ -- the heaviest hadron propagator yet observed. The choice $M \tilde{=} m_\rho$ is ruled out. If the charmed quark mass is approximately half of the ψ mass, the kinematics of photon-gluon-fusion[3] produce a Q^2-dependence similar to that in VMD. Data like that in Fig. 2 may provide a critical test of more exact QCD calculations.

We appreciate the strong support of Fermilab and its Neutrino Department, and the early participation of Drs. R. Cester and E. Groves. The excellent support groups at the collaborating institutions made fundamental contributions. This work was supported by the High Energy Physics Division of the U.S. Department of Energy under contract Nos. W-7405-Eng-48, EY-76-C-02-3072, EY-76-C-02-3000.

References

[1]Reviewed by T. Bauer et al., Rev. Mod. Phys. 50, 261 (1978).

[2]Reviewed by S.C.C. Ting, Rev. Mod. Phys. 49, 235 (1977); B. Richter, Rev. Mod. Phys. 49, 251 (1977).

[3]M. Glück and E. Reya, Phys. Lett 79B, 453 (1978); M. Glück and E. Reya, DESY preprint 79/05 (1979). In Fig. 2(c) we have multiplied their result for σ by 2.4 to obtain $d\sigma/dt(t=0)$.

[4]J.P. Leveille and T. Weiler, Nucl. Phys. B147, 147 (1979).

[5]V. Barger, W.Y. Keung, and R.J.N. Phillips, Univ. of Wisconsin preprint C00-881-83 (1979).

[6]B. Knapp et al., Phys. Rev. Lett. 34, 1040 (1975); W.Y. Lee, in Proc. Int. Symp. on Lepton and Photon Interactions at High Energies (DESY, Hamburg, 1977); M. Binkley, private communication.

[7]T. Nash et al., Phys. Rev. Lett. 36, 1233 (1976).

[8]U. Camerini et al., Phys. Rev. Lett. 35, 483 (1975).

[9]B. Gittelman et al., Phys. Rev. Lett. 36, 1616 (1975).

[10]G. Gollin, M.V. Isaila, F.C. Shoemaker, and P. Surko, IEEE Trans. Nuc. Sci. NS-26, 59 (1979).

[11]Use of the full sample for normalization reduces the cross section by less than one standard deviation.

[12]L.N. Hand, Phys. Rev. 129, 1834 (1963). Fig. 2c(2d) uses the $Q^2(\nu)$ dependence of the photon cross section given by the solid line in Fig. 2d(2c).

[13]See, for example, A. Silverman, in Proc. Int. Symp. on Electron and Photon Interactions at High Energies (Daresbury, 1969), Table 2.

[14]W.R. Ditzler et al., Phys. Lett. 57B, 201 (1975).